Journal of Molecular Graphics and Modelling 61 (2015) 13–20

Contents lists available at ScienceDirect

Journal of Molecular Graphics and Modelling

journal homepage: www.elsevier.com/locate/JMGM

Removal of a hazardous heavy metal from aqueous solution using functionalized graphene and boron nitride nanosheets: Insights from simulations

Jafar Azamat[a], Batoul Shirforush Sattary[a], Alireza Khataee[a,*], Sang Woo Joo[b,**]

[a] Research Laboratory of Advanced Water and Wastewater Treatment Processes, Department of Applied Chemistry, Faculty of Chemistry, University of Tabriz, 51666-16471 Tabriz, Iran
[b] School of Mechanical Engineering, Yeungnam University, 712-749 Gyeongsan, South Korea

ARTICLE INFO

Article history:
Received 7 April 2015
Received in revised form 19 May 2015
Accepted 20 June 2015
Available online 29 June 2015

Keywords:
Graphene
Boron nitride nanosheet
Potential of mean force
Heavy metal
Nanostructured membrane

ABSTRACT

A computer simulation was performed to investigate the removal of Zn^{2+} as a heavy metal from aqueous solution using the functionalized pore of a graphene nanosheet and boron nitride nanosheet (BNNS). The simulated systems were comprised of a graphene nanosheet or BNNS with a functionalized pore containing an aqueous ionic solution of zinc chloride. In order to remove heavy metal from an aqueous solution using the functionalized pore of a graphene nanosheet and BNNS, an external voltage was applied along the *z*-axis of the simulated box. For the selective removal of zinc ions, the pores of graphene and BNNS were functionalized by passivating each atom at the pore edge with appropriate atoms. For complete analysis systems, we calculated the potential of the mean force of ions, the radial distribution function of ion–water, the residence time of ions, the hydrogen bond, and the autocorrelation function of the hydrogen bond.

1. Introduction

A hazardous material is any agent that has the potential to harm humans, or the environment, if it is used or released improperly. Heavy metals (e.g., zinc ions) are considered hazardous materials. Zinc ions are discharged by electroplating, metalworking, galvanization, paint, batteries, smelting, fertilizers and pesticides, pigments, and the mining and steel processing industries [1]. A high level expression of zinc can cause human health disorders such as stomach cramps, skin irritations, vomiting, nausea, and anemia. The current regulation of wastewater and drinking water standards require that heavy metal contamination be reduced to a few parts per million [2].

Chemical precipitation, coagulation, ion exchange, adsorption, and reverse osmosis have been used for the removal of heavy metals [3–6]. Nanosheet membranes have also been used for the removal of various heavy metals [7]. Nanosheet membranes have the ability to separate ions and molecules. Ion separation using nanosheet membranes is done via pores created in them [8]. Graphene and boron nitride nanosheet (BNNS) are examples of nanostructured membranes.

Graphene is a two-dimensional (2-D) carbon-based nanomaterial with layers of carbon atoms densely packed in a honeycomb crystal lattice composed of two equivalent carbon sub-lattices [9]. Graphene offers a wide range of possible membrane applications because of its ultimate thinness, flexibility, chemical stability, and mechanical strength [10]. Since its recent isolation [11], graphene has been the subject of many exciting experimental [12–16] and theoretical studies [17]. The interaction of a graphene surface with target molecules results in an interesting material for water treatment applications.

Recently, ion permeation and gas separation through graphene membranes via the molecular dynamics (MD) simulation method have been performed [18–21]. MD simulations demonstrate that single-layer graphene with sub-nanometer-sized pores can be efficiently utilized for ion, gas, and hazardous ion separation [22–24].

In this work, along with graphene nanosheet, BNNSs were used for the removal of zinc ions. A BNNS with a very high specific surface area exhibits excellent sorption performance for a wide range of oils, solvents, and dyes from water [25]. This nanostructured material has unique properties compared to graphene, including a wide energy band gap, electrical insulation, ultraviolet photolumines-

* Corresponding author. Fax: +98 41 33340191.
** Corresponding author.
E-mail addresses: a_khataee@tabrizu.ac.ir (A. Khataee), swjoo@yu.ac.kr (S.W. Joo).

http://dx.doi.org/10.1016/j.jmgm.2015.06.012
1093-3263/

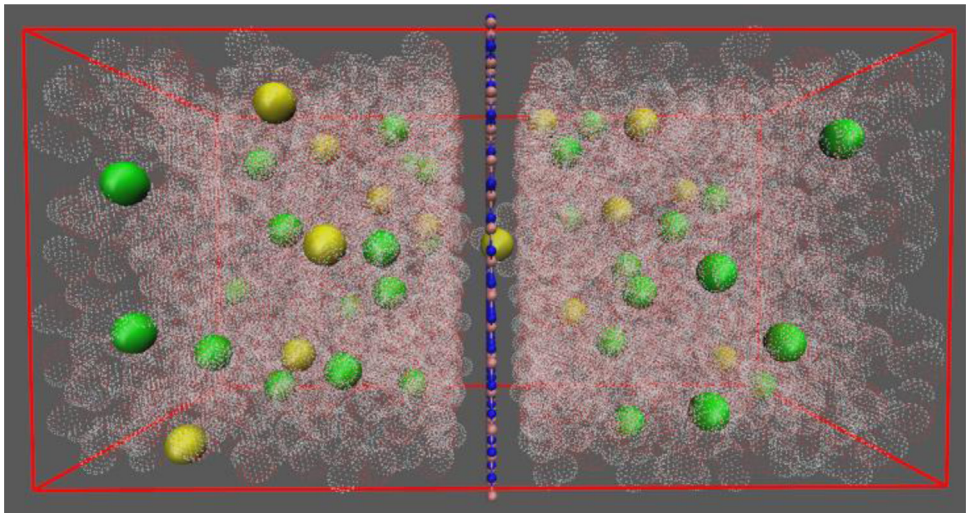

Fig. 1. The simulated system. The size of the box is $30 \times 30 \times 60$ Å^3. The BNNS membrane is located in the middle of simulation box (red represents O, white is H, yellow is Zn^{2+}, and green is Cl^-). (For interpretation of the references to color in this figure legend, the reader is referred to the web version of this article.)

cence, high thermal conductivity and stability, and high resistance to oxidation and chemical inertness [26–31]. The reusability of a saturated BNNS by burning in air, due to its high resistance against oxidation, is one of its important characteristics. This easy recyclability makes porous boron nitride nanosheet a good candidate for water treatment processes [25]. Perfect BNNS is impermeable to ions because there are no pores, and the electron density of its aromatic rings is enough to repel ions trying to pass through it. To pass ions through a BNNS, the drilling of pores is required. Functionalized pores in a BNNS are obtained by passivating each nitrogen and boron atom at the pore edge using chemical functional groups such as fluorine and hydrogen atoms. A functionalized BNNS can be used for the separation of heavy metals from water.

In this research, a molecular dynamics simulation of zinc ion separation from an aqueous solution using a graphene nanosheet and BNNS with a functionalized pore in its center was performed. We investigated a mechanism for ion separation based on the external voltage applied to the simulated system. To the best of our knowledge, no study has been reported in the literature on the removal of zinc ions by functionalized graphene nanosheet and BNNS. We expect that our findings can be used to aid the design of nanostructured membranes for the removal of hazardous materials for water treatment.

2. Simulation model and method

We used the MD simulation method to study the removal of heavy metals through the pores of graphene nanosheet and BNNS with various patterns. The MD simulation method is a valuable tool that is used to study of the permeation phenomenon if the permeation barrier is low enough to allow a sufficient number of crossings within the simulation time frame [32]. Fig. 1 shows an image of the simulation system. The size of the simulation box was $30 \times 30 \times 60$ Å^3. The box contained 1600 water molecules, with 0.5 M $ZnCl_2$ and a graphene nanosheet and BNNS as a nanostructured membrane in the middle of the box. The full geometric optimization of a functionalized graphene nanosheet and BNNS was calculated by using the density functional theory (DFT) method to obtain atomic charges and their optimized structures. The DFT method was performed using the GAMESS-US package [33] at the B3LYP level of theory using 6-311G basis sets. A repeated nanosheet unit was used for optimization of the functionalized membranes by the DFT method. The results from DFT calculations for the functionalized membranes are given in Table 1.

The dimensions of the membranes were 30×30 Å^2. There were 377 carbon atoms and 9 fluorine atoms in the graphene, and 183 nitrogen, 183 boron, 6 fluorine, and 6 hydrogen atoms in the BNNS (see Fig. 2). During the simulations, these membranes were held fixed. Graphene one of the the strongest materials with an intrinsic tensile strength of 130 GPa and a Young's modulus (stiffness) of 1 TPa [34]. Also, BNNS has the intrinsic tensile strength of 102 GPa and the Young's modulus of 145 Gpa [35]. So, we believe that graphene and BNNS membranes will be stable and the use of external high voltage does not affect their membranes.

The diameter of the pores in the graphene nanosheet and BNNS were about 6 and 8 Å, respectively. The pore diameter was determined from the open pore area measurements using the formula $d = 2\sqrt{A/\pi}$. These diameters of the pores were the most appropriate for our purpose. In this study, variants of the functionalized pores with different sizes were evaluated. But they did not have the desired selectivity. In addition to fluorine and hydrogen atoms used in this work, other atoms were investigated for pore functionalization. In this case, the best choice with a high-performance was functionalized pore with fluorine and hydrogen atoms.

The system was subjected to a zero-temperature energy minimization for 1 ns, and then the system temperature was increased to 298 K. After these steps, MD simulations were performed for 5 ns at 298 K under applied voltage before data collection. The voltage range from 0 to 35 V was used in this study. In the experimental works, many methods have been used for the removal of heavy metals; such as chemical precipitation, ion exchange, adsorption, and membrane filtration [36]. The range of voltage used in our MD study is similar to other experimental studies in which the voltage is used to remove heavy metals [37,38].

Table 1
Results obtained from DFT calculations for partial charges of graphene and BNNS atoms.

Atom type	Charge
Nitrogen	−0.4
Boron	0.4
Nitrogen bonded to fluorine	0.25
Boron bonded to hydrogen	0.05
Fluorine of BNNS	−0.25
Hydrogen of BNNS	−0.05
Carbon	0
Carbon bonded to fluorine	0.29
Fluorine of graphene	−0.29

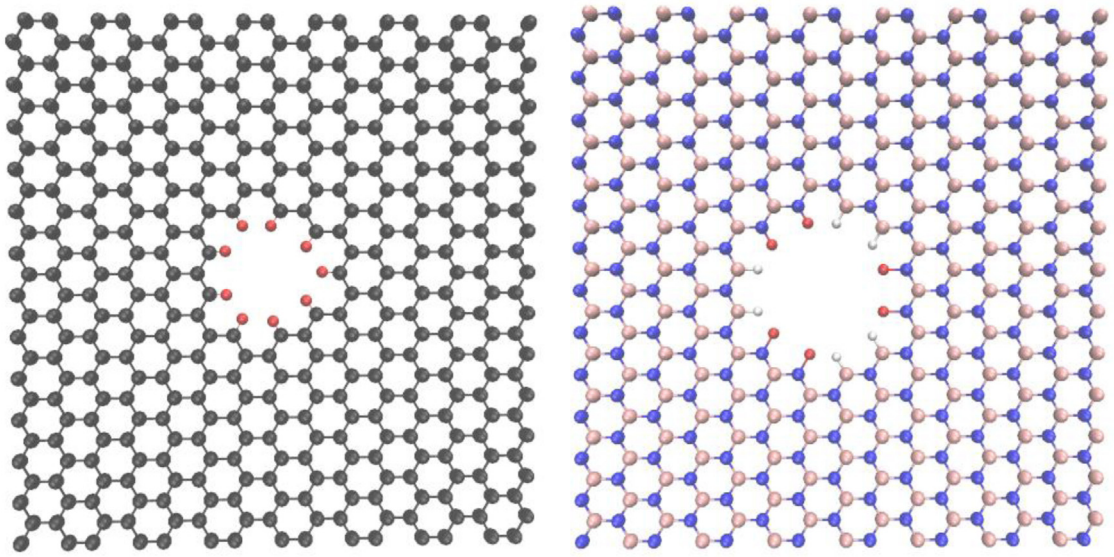

Fig. 2. Functionalized membranes. (a) Graphene (black represents carbon and red is fluoride). (b) BNNS (blue represents nitrogen, silver is boron, red is fluoride, and white is hydrogen). (For interpretation of the references to color in this figure legend, the reader is referred to the web version of this article.)

All MD simulations were carried out at constant volume using the NAMD 2.9 [39] package with the CHARMM27 force field [40] with periodic boundary conditions, a 1 fs time step at constant pressure (1 bar), and a temperature of 298 K.

A Langevin thermostat and a hybrid Nose–Hoover Langevin piston were used to maintain the temperature and pressure of the system at 298 K and 1 bar, respectively. The TIP3P water model [41] was used for the water molecules. This water model has superior diffusion and dielectric properties over standard three-site models, and is thus more suitable for treating water molecules in the membrane interior. The particle mesh Ewald method [42] was used to treat the long-range electrostatic interactions. In this research, as in previous works [43–48], all analyses were performed using VMD 1.9.2 software [49].

The effective potential energy (U_E) of the intermolecular interactions is given by the sum of the Coulomb potentials (U_C) and Lennard-Jones potentials (U_{vdw}) for long range and short range interactions, respectively, as follows [50]:

$$U_E = U_C + U_{vdw} = \frac{q_i \times q_j}{4\pi\epsilon_0 r_{ij}} + 4\sqrt{\epsilon_i \epsilon_j}\left[\left(\frac{(\sigma_i+\sigma_j)}{2r_{ij}}\right)^{12} - \left(\left(\frac{(\sigma_i+\sigma_j)}{2r_{ij}}\right)\right)^{6}\right] \quad (1)$$

where q_i and q_j represent the partial charge assigned to atoms i and j, respectively; r_{ij} refers to the distance between atoms i and j; and ϵ_i and σ_i represent the Lennard-Jones parameters. The U_{vdw} potential has its minimum $U_{min} = -\epsilon$ at a distance of $r = \sqrt[6]{2}\sigma$. Due to its simple form, the U_{vdw} potential is often used to describe the cross interaction of two different species. The interaction potentials of species i and j are first fitted to Lennard-Jones potentials. Then, the cross interaction Lennard-Jones parameters between species, ϵ_{ij} and σ_{ij}, can be calculated using the Lorenz-Berthelot combining rules:

$$\epsilon_{ij} = (\epsilon_i \epsilon_j)^{0.5} \text{and} \sigma_{ij} = \frac{1}{2}(\sigma_i + \sigma_j) \quad (2)$$

where ϵ_i, σ_i and ϵ_j, σ_j are the Lennard-Jones parameters for interactions occurring between species i and j, respectively [51,52]. The force field parameters for graphene were obtained from Sint et al. [53], and parameters for BNNS atoms were taken from Boldrin et al. [54].

During the simulation, an external voltage was applied to the system that was perpendicular to the pore of the membranes. In the pore of the graphene, fluorine atoms were used to passivate its carbon atoms. In the pore of the BNNS, hydrogen and fluorine atoms were used to passivate its boron and nitrogen atoms, respectively.

The ion permeation from functionalized pores can be explained by calculating the potential of the mean force (PMF) [55]. PMF

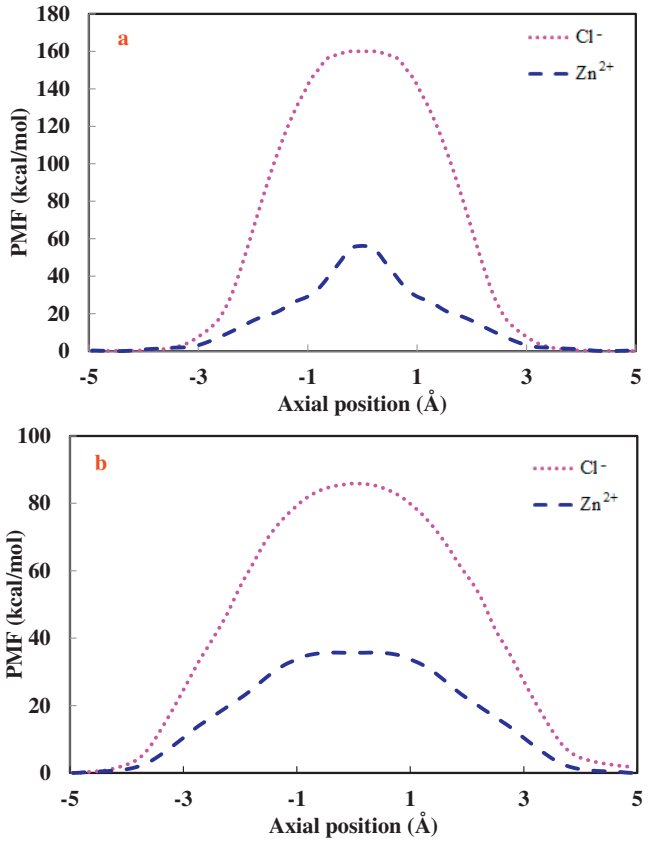

Fig. 3. The potential of the mean force for Zn^{2+} and Cl^- ions in: (a) graphene system, (b) BNNS system.

shows the probability of encountering the ion at a certain situation along the reaction coordinate, compared to encountering the ion in the bulk phase. The PMF was calculated by sampling the force experienced by ions that were placed at several positions along the *z*-axis of the box. In this work, each sampling window was run for 1 ns.

The PMF of the ions was calculated using umbrella sampling [56] with either ion harmonically restrained in 0.1 Å steps in the axial *z* direction (from −5 Å to 5 Å) with a force constant of 12.5 kcal/mol Å^2. Collective analysis was made using the weighted histogram analysis (WHAM) method [57]. WHAM is a general method that is used to combine data from multiple simulations in order to obtain thermodynamic properties of a given system. WHAM is often used to obtain the PMF from histograms of the reaction coordinate collected from multiple simulations of a system.

3. Results and discussion

To investigate the heavy metal removal phenomenon, we used the MD simulation method. The system examined in this work included Zn^{2+} as a heavy metal and a graphene nanosheet and BNNS as a membrane with a functionalized pore. External voltage was applied to the system that was perpendicular to the pore of the membranes. Under the influence of this voltage, a zinc ion permeates from the functionalized pore of the membranes. Although, the functionalized pores of graphene and BNNS have a radius large enough to accept zinc and chlorine ions, the MD results show that only Zn^{2+} permeates through these pores above a certain voltage.

The removal of heavy metal using nanostructured membranes can be clarified by calculating the PMF of ions. To investigate

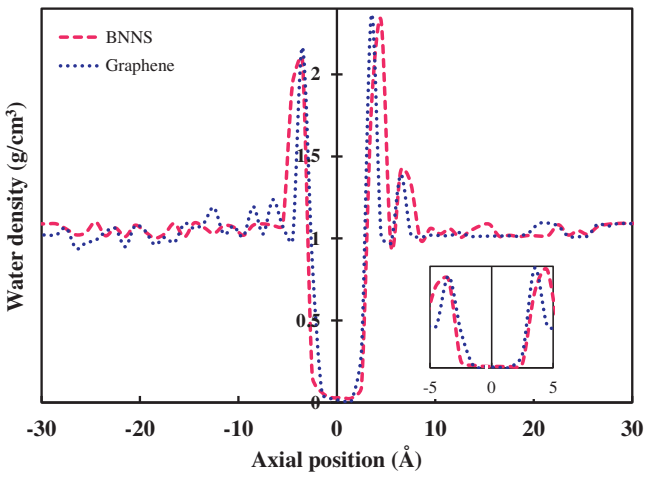

Fig. 4. Density profile of water molecules in the simulated system. Red line is for BNNS system and blue line is for graphene system. (For interpretation of the references to color in this figure legend, the reader is referred to the web version of this article.)

passage of ions in the absence of a voltage, we done 40 ns MD simulation without applied voltage. In this simulation, zinc and chloride ions did not pass through the functionalized pores. Therefore, we applied voltage–passage of ions from the pores. The PMF calculations cannot precisely predict the amount of voltage required to pass ions through a specific path. But PMF can predict passing or rejecting of a species through a species path. Fig. 3 shows the PMF for Zn^{2+} and Cl^- in the graphene (Fig. 3(a)) and BNNS (Fig. 3(b)).

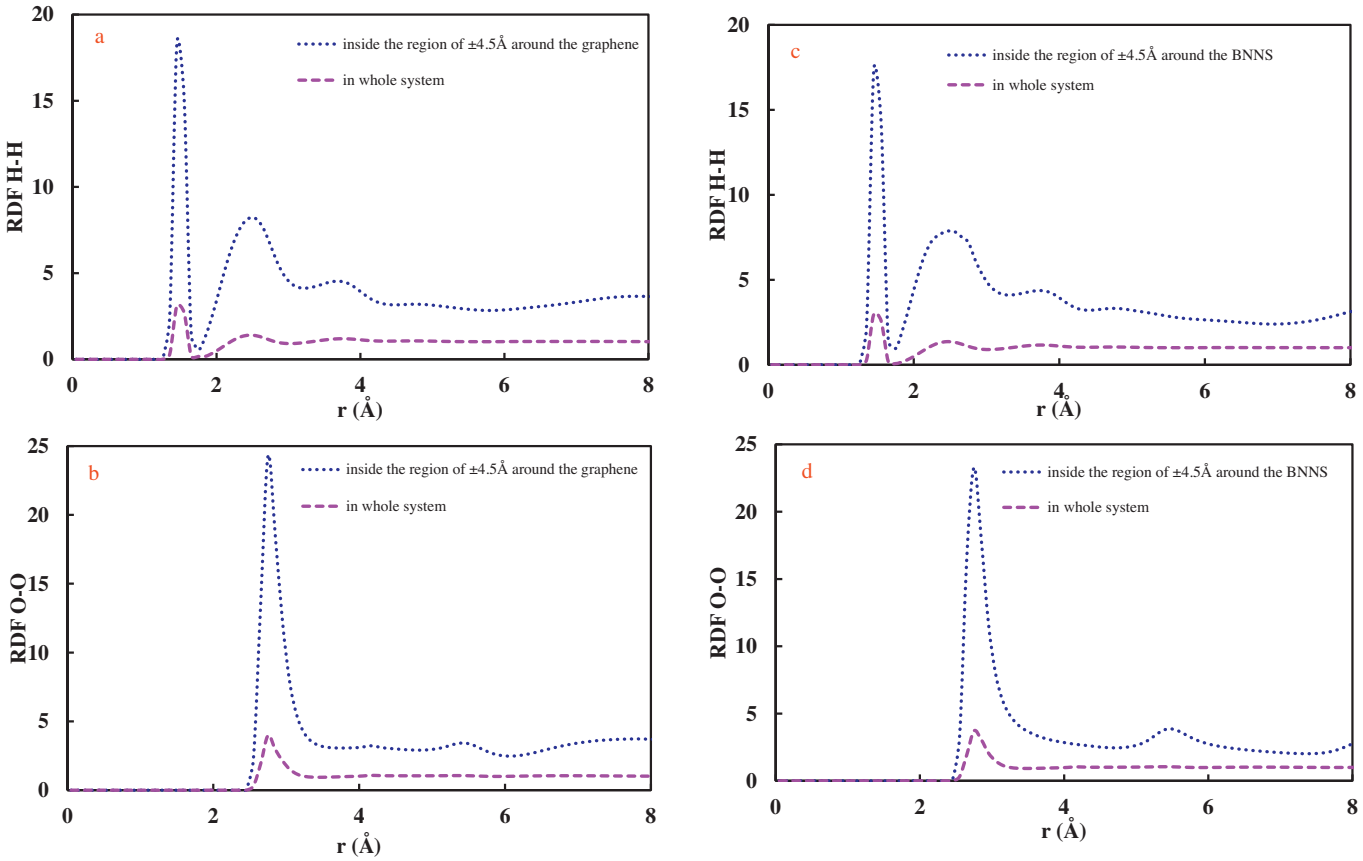

Fig. 5. Radial distribution functions of HH atoms and OO atoms of water molecules: (a) RDF HH in the graphene system, (b) RDF OO in the graphene system, (c) RDF HH in the BNNS system, and (d) RDF OO in the BNNS system.

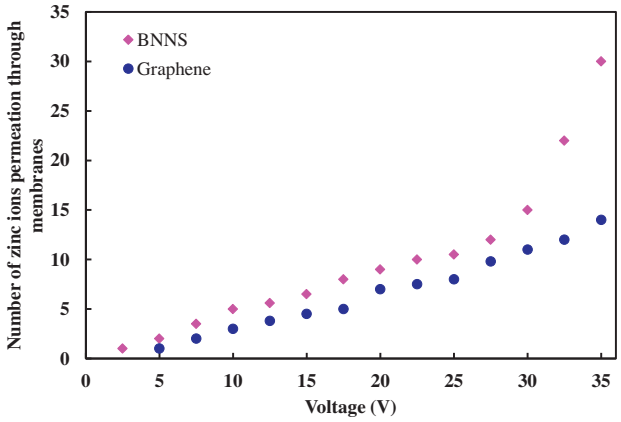

Fig. 6. The number of Zn^{2+} ions passing through the functionalized pore of graphene and BNNS membranes.

As can be seen, the energy barrier for Cl^- is higher than that of Zn^{2+} in both membranes. Thus, the chloride ion will not be able to cross the membrane. This restriction occurs because the functionalized pores are terminated by the negatively-charged atoms, which favors the passage of cations. Also, the energy barrier for Zn^{2+} in the graphene nanosheet is higher than that of the BNNS. This phenomenon leads to more heavy metal permeating from the pore of the BNNS membrane. We note that the ion permeation occurs only in the presence of an external voltage. The passing of ions from pores would not have occurred if the voltage had not been applied. The Zn^{2+} permeated from functionalized pores when 5 and 2.5 V electric fields were applied to the graphene and BNNS membranes, respectively.

The structure of water molecules in the simulated systems was studied. We calculated the water density profile and radial distribution functions (RDFs) between oxygen–oxygen and hydrogen–hydrogen water molecules inside a region of ±4.5 Å around the membrane, and in the whole system. In the simulated systems, the structure of water molecules was different from that of water molecules in the bulk region. Fig. 4 shows the water density profile in the simulated systems. The density profile was calculated from histograms of the number of water molecules. The water molecules displayed a tendency to accumulate in the region at a location about ±4.5 Å from the graphene nanosheet and BNNS. In fact, the density of water on both sides of the membranes was higher than that in the bulk water. This phenomenon occurred for both types of membranes. This structure is shown by two peaks visible in the density profile on each side. In the region far away from the membranes, the density of water was about 1 g/cm^3. These observations were confirmed by calculating the RDFs between atoms of water molecules (oxygen–oxygen and hydrogen–hydrogen) inside a region ±4.5 Å around the membranes, and in the whole system (see Fig. 5). In this region, the intensity of the RDF peak between H–H and O–O of the water molecules is higher than that of the whole system. The layered structure of water molecules in this region is due to the non-bonded interaction of membranes atoms, and water molecules.

Fig. 6 presents the number of heavy metals passing across the functionalized pore of the membranes (graphene nanosheet and BNNS). As the applied voltage increases, the number of heavy metals passing from the pore of the membranes increases. As seen in Fig. 6, zinc ions pass through the pore of the BNNS more easily than through the pore of the graphene nanosheet. This is due to the low energy barrier of Zn^{2+} in the BNNS compared to that in the graphene (see the PMF of ions in Fig. 3).

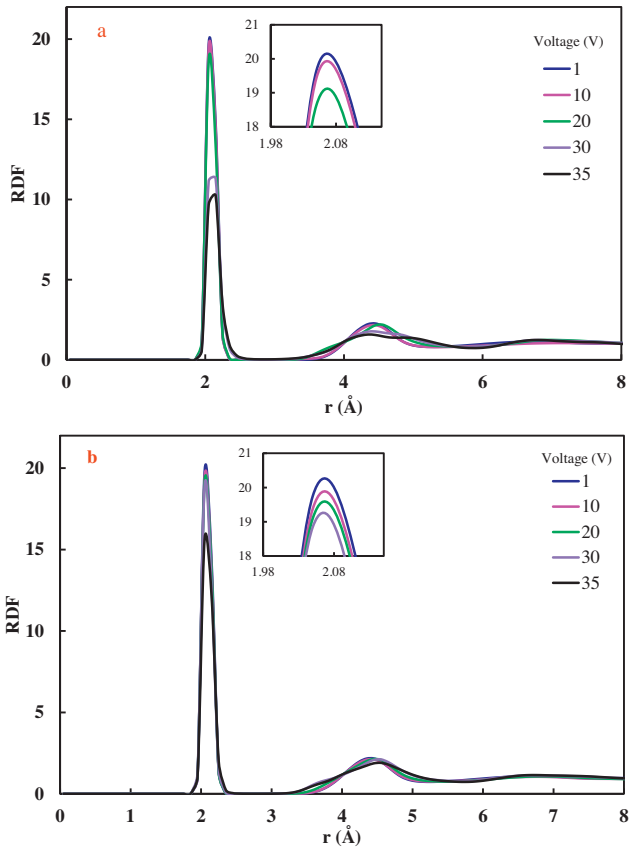

Fig. 7. RDFs of ion–oxygen in the simulation box under various voltages: (a) RDF Zn^{2+}–oxygen in the graphene system, (b) RDF Zn^{2+}–oxygen in the BNNS system.

To characterize the structure of water molecules around the ions in the simulation box, the RDF ($g(r)$) between the ion and water molecule was obtained from the trajectory files of the 5 ns MD simulation. The ion-water RDF describes the probability density of finding a particle at a distance r from a given particle position. There is an obvious first maximum and minimum for each RDF peak. These show that a coordination shell of ions exists inside the water box. Fig. 7 represents the RDF Zn^{2+}–oxygen atom of water in both systems. The first peak of the RDF corresponds to the distribution of the first neighbor water molecules around the considered ion. The first minimum in the ion–water RDF is at a distance of 2.45 Å and 2.35 Å in the graphene nanosheet and BNNS, respectively; this is the effective size of the complex (composed of the ion and first neighbor water molecules). For the RDF peaks of zinc ions in the graphene nanosheet and BNNS systems, the position and magnitude of the first maximum and minimum are almost identical. This indicates that the hydration number of this ion in both systems is identical.

To study the ions passing through the functionalized pores of membranes, the residence times of the zinc ion was also investigated. The residence time is the amount of time required for an ion to pass through the pore. Fig. 8 shows the residence time of a zinc ion as a function of applied voltage. Increasing the voltage decreases the residence time. Therefore, removal of zinc ions from the aqueous solution at high voltages happens quickly. The energy barrier in the PMF for Zn^{2+} in the graphene pore is high compared to that of the BNNS pore. Thus, the residence time of the zinc ion in the graphene system is greater than that of the BNNS system. Therefore, Zn^{2+} passes quickly through the pore of the BNNS membrane.

In these membranes, when water molecules pass through the functionalized pores, they form a single file structure. Fig. 9(a)

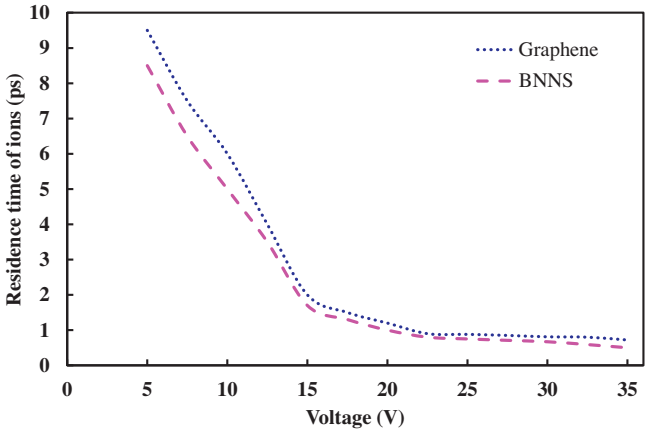

Fig. 8. Residence time for Zn^{2+} ions at the applied voltages in the graphene and BNNS systems.

shows the number of average hydrogen bonds between water molecules at the applied voltages. The number of hydrogen bonds was calculated with VMD software using the structure characteristics of hydrogen bonds during the simulation. As Fig. 9(a) shows the number of hydrogen bonds increases as the voltage increases. Furthermore, the dynamics of the hydrogen bonds of water molecules can be explained by using the autocorrelation function of the hydrogen bonds (ACFHB) of the water molecules [58]. This parameter is written as follows:

$$\mathrm{ACFHB}(t) = \frac{\langle h(0) \times h(t) \rangle}{\langle h \rangle} \tag{3}$$

where $h(t)$ is the hydrogen bond population operator for each pair of water molecules, and has a value of 1 if a hydrogen bond is present at time t between two tagged water molecules, or zero if a hydrogen bond is not present [59]. The $\langle h \rangle$ is the average of $h(t)$. The ACFHB indicates the conditional probability that the tagged pair of water molecules forms hydrogen bonding at time t given that the pair was hydrogen bonded at time zero. It shows how fast the hydrogen bonds of the systems relaxed. A faster decrease of ACFHB in the membranes indicates that the hydrogen bonds of water molecules are relatively weak and broken frequently (see Fig. 9(b) and (c)). In both systems, this decreasing trend is intensified with a reduction in the applied voltage.

As seen in the Fig. 7 (RDF graphs), surrounding structure of Zn ions is almost identical in both graphene and BNNS systems. Also, the structure of water molecules around the membranes in both systems is similar (Fig. 4). The water molecules displayed a ten-

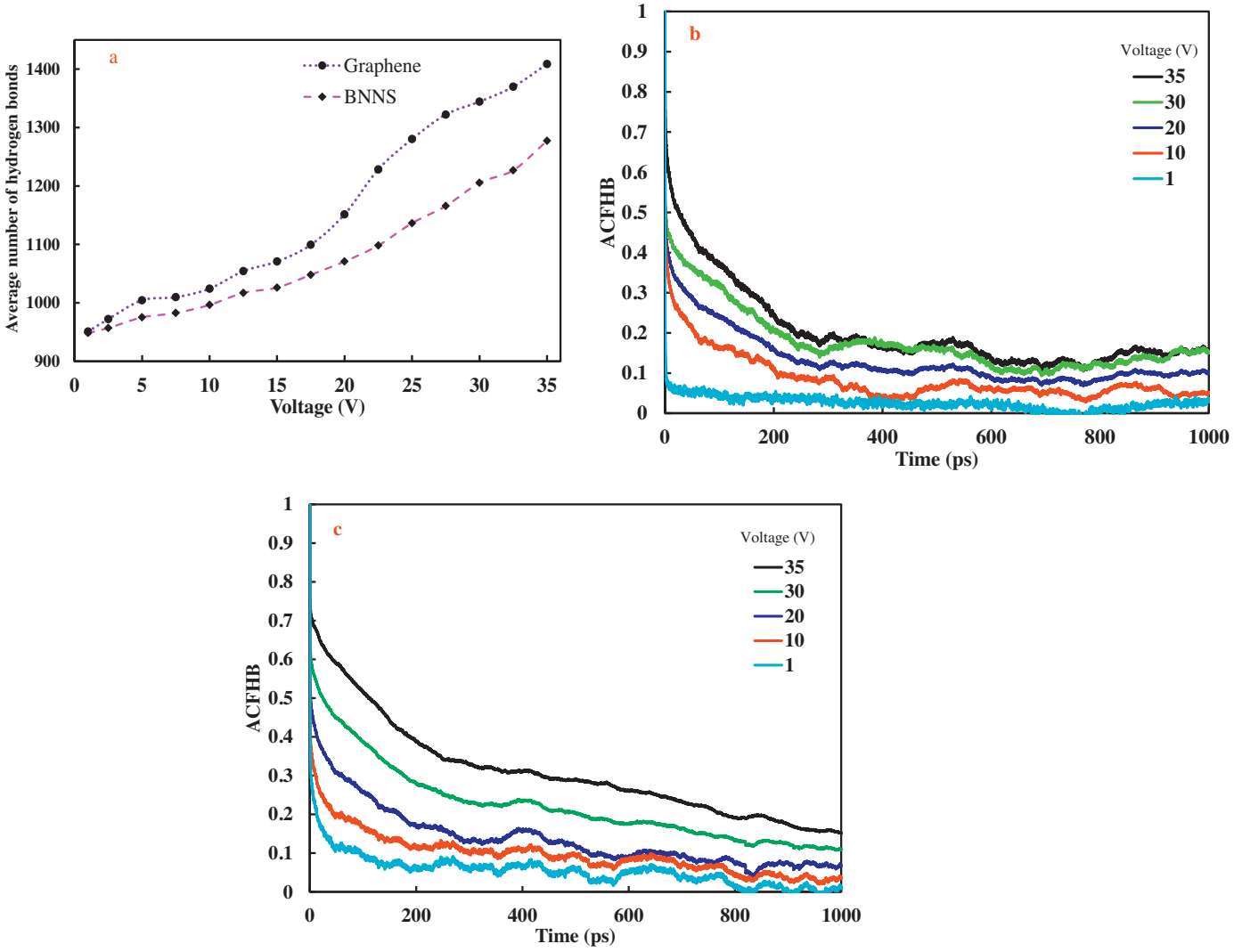

Fig. 9. (a) Average number of hydrogen bonds between water molecules at the applied voltages. Autocorrelation functions of hydrogen bonds at the applied voltages in (b) the graphene system and (c) the BNNS system.

dency to accumulate in the region at a location about ±4.5 Å from the graphene nanosheet and BNNS. This phenomenon occurred for both types of the membranes. This structure is shown by two peaks visible in the density profile on each side. These observations were confirmed by calculating the RDFs between atoms of water molecules (oxygen–oxygen and hydrogen–hydrogen) inside a region ±4.5 Å around the membranes, and in the whole system (Fig. 5). However, the number of zinc ions passing through the graphene and BNNS is different. This indicates that structure of the water molecules were ineffective in the number of ions passing through the functionalized pores. Therefore, difference in number of ions passing through the pores is related to the pore structure. This case is illustrated by the PMF graphs, in which the barrier energy of Zn ions in the BNNS is less than that of graphene. Thus, the residence time of the zinc ions in the BNNS system is less than that of the graphene system. Therefore, Zn^{2+} passes quickly through the pore of the BNNS membrane.

4. Conclusion

We used MD simulations to study the permeation of a heavy metal through nanostructured membranes. We used two membranes for this purpose: graphene nanosheet and BNNS. First, the centres of these membranes were perforated and then functionalized with appropriated atoms. Based on the results of our PMF calculations, the graphene and BNNS were able to remove zinc ions from aqueous solutions. Compared to the graphene nanosheet, a BNNS can remove the heavy metal from water efficiently. With increasing applied voltage to the considered systems, more ions could pass through the membranes. In addition, with increasing applied voltage, the residence time of the ions decreased. In the simulated systems, the water molecules displayed a tendency to accumulate in a region located about ±4.5 Å from the graphene or BNNS. This behaviour was confirmed by calculating the density profile and RDF.

Acknowledgments

We thank the University of Tabriz and Iranian Nanotechnology Initiative Council for the support provided.

References

[1] C. Gakwisiri, N. Raut, A. Al-Saadi, S. Al-Aisri, A. Al-Ajmi, A critical review of removal of zinc from wastewater, Proceedings of the World Congress on Engineering, in: July 4–6, London, U.K., 1, 2012, p. 627.
[2] M. Parmar, L.S. Thakur, Heavy metal Cu, Ni and Zn: toxicity, health hazards and their removal techniques by low cost adsorbents: a short overview, Int. J. Plant Anim. Environ. Sci. 3 (2013) 143–157.
[3] H.A. Hegazi, Removal of heavy metals from wastewater using agricultural and industrial wastes as adsorbents, HBRC J. 9 (2013) 276–282.
[4] S. Štandeker, A. Veronovski, Ž. Novak, Ž. Knez, Silica aerogels modified with mercapto functional groups used for Cu(II) and Hg(II) removal from aqueous solutions, Desalination 269 (2011) 223–230.
[5] A.K. Meena, G.K. Mishra, P.K. Rai, C. Rajagopal, P.N. Nagar, Removal of heavy metal ions from aqueous solutions using carbon aerogel as an adsorbent, J. Hazard. Mater. 122 (2005) 161–170.
[6] G. Chen, Electrochemical technologies in wastewater treatment, Sep. Purif. Technol. 38 (2004) 11–41.
[7] P.S. Goh, A.F. Ismail, Graphene-based nanomaterial: the state-of-the-art material for cutting edge desalination technology, Desalination 356 (2015) 115–128.
[8] M.E. Suk, N.R. Aluru, Water transport through ultrathin graphene, J. Phys. Chem. Lett. 1 (2010) 1590–1594.
[9] Z. He, J. Zhou, X. Lu, B. Corry, Bioinspired graphene nanopores with voltage-tunable ion selectivity for Na^+ and K^+, ACS Nano 7 (2013) 10148–10157.
[10] F. Taherian, V. Marcon, N.F.A. van der Vegt, F. Leroy, What is the contact angle of water on graphene? Langmuir 29 (2013) 1457–1465.
[11] C.Ö. Girit, J.C. Meyer, R. Erni, M.D. Rossell, C. Kisielowski, L. Yang, C.-H. Park, M.F. Crommie, M.L. Cohen, S.G. Louie, A. Zettl, Graphene at the edge: stability and dynamics, Science 323 (2009) 1705–1708.
[12] J. Wu, L. Xie, Y. Li, H. Wang, Y. Ouyang, J. Guo, H. Dai, Controlled chlorine plasma reaction for noninvasive graphene doping, J. Am. Chem. Soc. 133 (2011) 19668–19671.
[13] D.W. Boukhvalov, M.I. Katsnelson, Chemical functionalization of graphene, J. Phys. Condens. Matter 21 (2009) 344205.
[14] M.Z. Hossain, J.E. Johns, K.H. Bevan, H.J. Karmel, Y.T. Liang, S. Yoshimoto, K. Mukai, T. Koitaya, J. Yoshinobu, M. Kawai, A.M. Lear, L.L. Kesmodel, S.L. Tait, M.C. Hersam, Chemically homogeneous and thermally reversible oxidation of epitaxial graphene, Nat. Chem. 4 (2012) 305–309.
[15] B. Huang, Z. Li, Z. Liu, G. Zhou, S. Hao, J. Wu, B.-L. Gu, W. Duan, Adsorption of gas molecules on graphene nanoribbons and its implication for nanoscale molecule sensor, J. Phys. Chem. C 112 (2008) 13442–13446.
[16] Q.H. Wang, M.C. Hersam, Room-temperature molecular-resolution characterization of self-assembled organic monolayers on epitaxial graphene, Nat. Chem. 1 (2009) 206–211.
[17] M. Klintenberg, S. Lebègue, M.I. Katsnelson, O. Eriksson, Theoretical analysis of the chemical bonding and electronic structure of graphene interacting with group IA and group VIIA elements, Phys. Rev. B: Condens. Matter 81 (2010) 085433.
[18] D. Konatham, J. Yu, T.A. Ho, A. Striolo, Simulation insights for graphene-based water desalination membranes, Langmuir 29 (2013) 11884–11897.
[19] D. Cohen-Tanugi, J.C. Grossman, Water desalination across nanoporous graphene, Nano Lett. 12 (2012) 3602–3608.
[20] L.W. Drahushuk, M.S. Strano, Mechanisms of gas permeation through single layer graphene membranes, Langmuir 28 (2012) 16671–16678.
[21] C. Sun, M.S.H. Boutilier, H. Au, P. Poesio, B. Bai, R. Karnik, N.G. Hadjiconstantinou, Mechanisms of molecular permeation through nanoporous graphene membranes, Langmuir 30 (2013) 675–682.
[22] M.E. Suk, N.R. Aluru, Ion transport in sub-5-nm graphene nanopores, J. Chem. Phys. 140 (2014).
[23] T.R. Gaborski, J.L. Snyder, C.C. Striemer, D.Z. Fang, M. Hoffman, P.M. Fauchet, J.L. McGrath, High-performance separation of nanoparticles with ultrathin porous nanocrystalline silicon membranes, ACS Nano 4 (2010) 6973–6981.
[24] D.E. Jiang, V.R. Cooper, S. Dai, Porous graphene as the ultimate membrane for gas separation, Nano Lett. 9 (2009) 4019–4024.
[25] W. Lei, D. Portehault, D. Liu, S. Qin, Y. Chen, Porous boron nitride nanosheets for effective water cleaning, Nat. Commun. 4 (2013) 1777.
[26] D. Golberg, Y. Bando, Y. Huang, T. Terao, M. Mitome, C. Tang, C. Zhi, Boron nitride nanotubes and nanosheets, ACS Nano 4 (2010) 2979–2993.
[27] B. Mortazavi, Y. Rémond, Investigation of tensile response and thermal conductivity of boron-nitride nanosheets using molecular dynamics simulations, Physica E 44 (2012) 1846–1852.
[28] W. Lei, H. Zhang, Y. Wu, B. Zhang, D. Liu, S. Qin, Z. Liu, L. Liu, Y. Ma, Y. Chen, Oxygen-doped boron nitride nanosheets with excellent performance in hydrogen storage, Nano Energy 6 (2014) 219–224.
[29] Q. Sun, Z. Li, D.J. Searles, Y. Chen, G. Lu, A. Du, Charge-controlled switchable CO_2 capture on boron nitride nanomaterials, J. Am. Chem. Soc. 135 (2013) 8246–8253.
[30] A. Pakdel, C. Zhi, Y. Bando, D. Golberg, Low-dimensional boron nitride nanomaterials, Mater. Today 15 (2012) 256–265.
[31] Y. Wang, Z. Shi, J. Yin, Boron nitride nanosheets: large-scale exfoliation in methanesulfonic acid and their composites with polybenzimidazole, J. Mater. Chem. 21 (2011) 11371–11377.
[32] S. Razavi, J. Koplik, I. Kretzschmar, Molecular dynamics simulations: insight into molecular phenomena at interfaces, Langmuir 30 (2014) 11272–11283.
[33] M.W. Schmidt, K.K. Baldridge, J.A. Boatz, S.T. Elbert, M.S. Gordon, J.H. Jensen, S. Koseki, N. Matsunaga, K.A. Nguyen, S. Su, T.L. Windus, M. Dupuis, J.A. Montgomery, General atomic and molecular electronic structure system, J. Comput. Chem. 14 (1993) 1347–1363.
[34] C. Lee, X. Wei, J.W. Kysar, J. Hone, Measurement of the elastic properties and intrinsic strength of monolayer graphene, Science 321 (2008) 385–388.
[35] H. Zhu, Y. Li, Z. Fang, J. Xu, F. Cao, J. Wan, C. Preston, B. Yang, L. Hu, Highly thermally conductive papers with percolative layered boron nitride nanosheets, ACS Nano 8 (2014) 3606–3613.
[36] F. Fu, Q. Wang, Removal of heavy metal ions from wastewaters: a review, J. Environ. Manage. 92 (2011) 407–418.
[37] K. Choi, T. Jeoung, Removal of zinc ions in wastewater by electrodialysis, Kor. J. Chem. Eng. 19 (2002) 107–113.
[38] E. Bazrafshan, A.H. Mahvi, M.A. Zazouli, Removal of zinc and copper from aqueous solutions by electrocoagulation technology using iron electrodes, Asian J. Chem. 23 (2011) 5506–5510.
[39] L. Kalé, R. Skeel, M. Bhandarkar, R. Brunner, A. Gursoy, N. Krawetz, J. Phillips, A. Shinozaki, K. Varadarajan, K. Schulten, NAMD2: greater scalability for parallel molecular dynamics, J. Comput. Phys. 151 (1999) 283–312.
[40] A.D. MacKerell, D. Bashford Bellott, R.L. Dunbrack, J.D. Evanseck, M.J. Field, S. Fischer, J. Gao, H. Guo, S. Ha, D. Joseph-McCarthy, L. Kuchnir, K. Kuczera, F.T.K. Lau, C. Mattos, S. Michnick, T. Ngo, D.T. Nguyen, B. Prodhom, W.E. Reiher, B. Roux, M. Schlenkrich, J.C. Smith, R. Stote, J. Straub, M. Watanabe, J. Wiórkiewicz-Kuczera, D. Yin, M. Karplus, All-atom empirical potential for molecular modeling and dynamics studies of proteins, J. Phys. Chem. B 102 (1998) 3586–3616.
[41] W.L. Jorgensen, J. Chandrasekhar, J.D. Madura, R.W. Impey, M.L. Klein, Comparison of simple potential functions for simulating liquid water, J. Chem. Phys. 79 (1983) 926–935.
[42] T. Darden, D. York, L. Pedersen, Particle mesh Ewald: an N·log(N) method for Ewald sums in large systems, J. Chem. Phys. 98 (1993) 10089–10092.

[43] J. Azamat, A. Khataee, S. Joo, Separation of a heavy metal from water through a membrane containing boron nitride nanotubes: molecular dynamics simulations, J. Mol. Model. 20 (2014) 1–9.
[44] J. Azamat, A. Khataee, S.W. Joo, Functionalized graphene as a nanostructured membrane for removal of copper and mercury from aqueous solution: a molecular dynamics simulation study, J. Mol. Graphics Modell. 53 (2014) 112–117.
[45] J. Azamat, J.J. Sardroodi, A. Rastkar, Water desalination through armchair carbon nanotubes: a molecular dynamics study, RSC Adv. 4 (2014) 63712–63718.
[46] J. Azamat, A. Khataee, S.W. Joo, Molecular dynamics simulation of trihalomethanes separation from water by functionalized nanoporous graphene under induced pressure, Chem. Eng. Sci. 127 (2015) 285–292.
[47] J. Azamat, A. Khataee, S.W. Joo, Removal of heavy metals from water through armchair carbon and boron nitride nanotubes: a computer simulation study, RSC Adv. 5 (2015) 25097–25104.
[48] J. Azamat, A. Khataee, S.W. Joo, B. Yin, Removal of trihalomethanes from aqueous solution through armchair carbon nanotubes: a molecular dynamics study, J. Mol. Graphics Modell. 57 (2015) 70–75.
[49] W. Humphrey, A. Dalke, K. Schulten, VMD: visual molecular dynamics, J. Mol. Graphics 14 (1996) 33–38.
[50] C.Y. Won, N.R. Aluru, Water permeation through a subnanometer boron nitride nanotube, J. Am. Chem. Soc. 129 (2007) 2748–2749.
[51] M. Alvarez, E. Lomba, C. Martín, M. Lombardero, Atom–atom structure factors of hydrogen halides: a molecular approach revisited, J. Chem. Phys. 103 (1995) 3680–3685.
[52] L. Viola, S. Lloyd, Dynamical suppression of decoherence in two-state quantum systems, Phys. Rev. A 58 (1998) 2733–2744.
[53] K. Sint, B. Wang, P. Kral, Selective ion passage through functionalized graphene nanopores, J. Am. Chem. Soc. 130 (2008) 16448–16449.
[54] L. Boldrin, F. Scarpa, R. Chowdhury, S. Adhikari, Effective mechanical properties of hexagonal boron nitride nanosheets, Nanotechnology 22 (2011) 505702.
[55] R. Kjellander, H. Greberg, Mechanisms behind concentration profiles illustrated by charge and concentration distributions around ions in double layers, J. Electroanal. Chem. 450 (1998) 233–251.
[56] G.M. Torrie, J.P. Valleau, Nonphysical sampling distributions in Monte Carlo free-energy estimation: umbrella sampling, J. Comput. Phys. 23 (1977) 187–199.
[57] S. Kumar, P.W. Payne, M. Vásquez, Method for free-energy calculations using iterative techniques, J. Comput. Chem. 17 (1996) 1269–1275.
[58] A. Luzar, Resolving the hydrogen bond dynamics conundrum, J. Chem. Phys. 113 (2000) 10663–10675.
[59] B. Bagchi, Water dynamics in the hydration layer around proteins and micelles, Chem. Rev. 105 (2005) 3197–3219.